How to cite: *Angew. Chem. Int. Ed.* **2024**, *63*, e202317553
doi.org/10.1002/anie.202317553

Host-Guest Chemistry

Delving into the Variability of Supramolecular Affinity: Self-Ion Pairing as a Central Player in Aqueous Host-Guest Chemistry

Borja Gómez-González, Nuno Basílio, Belén Vaz, Moisés Pérez-Lorenzo, and Luis García-Río**

Abstract: The determination of binding constants is a key matter in evaluating the strength of host–guest interactions. However, the profound impact of self-ion pairing on this parameter is often underrated in aqueous solution, leading in some cases to a misinterpretation of the true potential of supramolecular assemblies. In the present study, we aim to shed further light on this critical factor by exploring the concentration-dependent behavior of a multicharged pillararene in water. Our observations reveal an extraordinary 1-million-fold variability in the affinity of this macrocycle toward a given anion, showcasing the highly dynamic character of electrostatic interactions. We argue that these findings bring to the forefront the inherent determinism that underlies the estimation of affinity constants, a factor profoundly shaped by both the sensitivity of the instrumental technique in use and the intricacies of the experimental design itself. In terms of applications, these results may provide the opportunity to optimize the operational concentrations of multicharged hosts in different scenarios, aiming to achieve their maximum efficiency based on the intended application. Unlocking the potential of this hidden variability may pave the way for the creation of novel molecular materials with advanced functionalities.

[*] Dr. B. Gómez-González, Prof. L. García-Río
Department of Physical Chemistry,
Universidade de Santiago de Compostela
15782 Santiago de Compostela (Spain)
E-mail: luis.garcia@usc.es

Dr. N. Basílio
Laboratório Associado para a Química Verde (LAQV), Rede de Química e Tecnologia (REQUIMTE), Departamento de Química, Faculdade de Ciências e Tecnologia, Universidade NOVA de Lisboa
2829-516 Caparica (Portugal)

Dr. B. Vaz, Dr. M. Pérez-Lorenzo
CINBIO, Universidade de Vigo
36310 Vigo (Spain)
and
Galicia Sur Health Research Institute
36310 Vigo (Spain)
E-mail: moisespl@uvigo.es

Introduction

Over the years, supramolecular systems have gained increasing attention owing to their numerous applications, as these non-covalent assemblies are promising candidates for developing advanced materials,[1–4] drug delivery platforms,[5–8] sensors,[9–12] imaging agents,[13–16] and catalysts,[17–20] among other functional structures.[21–24] Host-guest complexes represent an essential subclass of these architectures, where a guest molecule selectively binds to a complementary host molecule forming a stable complex.[25] In this scenario, the host partner plays a pivotal role in controlling the properties and functions of the resulting assembly.[26] For this reason, a myriad of innovative host molecules has been synthesized, providing numerous options for constructing these supramolecular complexes.[27] Among these hosts, cyclodextrins,[28,29] cucurbiturils,[30–32] calixarenes,[33,34] and pillararenes,[35,36] stand out as highly adaptable macrocycles with diverse and tunable properties. These molecules have well-defined three-dimensional cavities that can be precisely tailored, allowing for the preferential recognition of specific guests.[37] This synthetic versatility is particularly important for applications that require the host to be soluble in aqueous environments,[38] especially in the biomedical field.[39,40] A common strategy to accomplish this goal is the incorporation of charged moieties at the portals of these receptors, which allows for an enhanced solubility in water.[41] In relation to this issue, multicharged macrocycles are an interesting group of host molecules due to their ability to selectively bind ionic guests.[42,43] These molecules are typically composed of multiple charged units, which create a cavity that is complementary in shape and charge to the guest ion.[25] The resulting host–guest complex is stabilized by a combination of electrostatic and other non-covalent interactions, thus leading to a high selectivity and affinity.[44]

The influence of counterions on the binding affinities of multicharged receptors in organic solvents has been studied in detail.[45–47] Nevertheless, this in-depth comprehension has yet to find its match in aqueous solutions, where counterions are often perceived to play a passive role.[48] As a consequence, polyionic supramolecular hosts have commonly been characterized in water by a fixed binding constant regardless of their concentration. Accordingly, under a set of predefined operational conditions, this value remains unchanged for a given guest and stoichiometry. In a way, the normalization of this concept is somewhat striking considering that altering the concentration of these multi-

charged hosts carries major implications on the degree of binding between these receptors and their ubiquitous counterions. It must be noted that for electrolyte-based species, concentration influences the extent of cation-anion interactions and, consequently, the propensity for either single ion or ion pair formation upon dissolution in water.[49] In this context, higher concentrations facilitate the assembly of ions into pairs, whereas lower concentrations promote the prevalence of free hydrated ions.[50] This delicate equilibrium between ion pairing and solvation profoundly influences the degree of ionization and therefore, several solution properties, including conductivity, activity coefficients, and diffusion constants.[51] In view of the abovementioned, the concentration of polyionic macrocycles is expected to directly correlate with the degree of formation of ion pairs or, in simpler terms, with the number of counterions bound to the charged moieties of these hosts. As a result, it is logical to assume that concentration must exhibit a negative correlation with the net charge of these receptors as the electric fields around the ion pairs are partially cancelled due to the opposite charge of its constituents. For this reason, it is crucial to give due consideration to the concentration of multicharged macrocycles since this factor may critically influence the strength of the electrostatic interactions in the supramolecular assemblies arising from the incorporation of ionic guests, thus affecting the equilibria defining the value of the complexation constant itself. This aspect gains even greater significance when considering the wide range of scenarios where these macrocycles can be employed. Concerning this issue, host concentrations can vary widely in terms of applications, ranging from minute quantities in supramolecular catalysis[52] to large-scale amounts as water pollutant adsorbents.[53] Hence, to ensure an optimal performance in all the different settings, understanding how the host affinities are influenced by the operational concentrations becomes imperative. Acquiring a deeper comprehension in this regard will not only enhance the reliability of the quantitative evaluation of the dynamics of supramolecular complexes, but it will also enable a more precise molecular design of the host depending on its intended application, thereby allowing to achieve its maximum efficiency in terms of guest encapsulation. In this context, earlier investigations delving into the influence of added salts, buffers, and to a lesser extent, the impact of counterions, have highlighted moderate yet noteworthy effects of these species on the thermodynamic and mechanistic features of host–guest complexes in aqueous environments.[54–58] It is also worth noting that these effects usually become relevant at added ionic strengths surpassing the millimolar range.

By merging experimental techniques and numerical methods, this study aims to extract valuable insights into the different ionization states that multicharged hosts may adopt depending on their concentration, and how these diverse configurations show dramatic differences in terms of affinity for a given guest. To accomplish this, a polycationic pillararene featuring ten charged functional groups is employed (Scheme 1). The proposed hypothesis on the hidden variability in the complexation capacity of these hosts is thus substantiated, highlighting the need of incorporating this variable for both the molecular design and the applications of these macrocycles. The findings derived from this investigation call for a critical reassessment of the existing data pertaining to these hosts, emphasizing the need of specifying concentration as a key element while reporting the complexation ability of these multicharged supramolecular receptors.

Results and Discussion

As a starting point, pillar[5]arene (P5A) is synthesized using well-established procedures reported in the literature.[59] Perfunctionalization of pillar[n]arenes has emerged as an

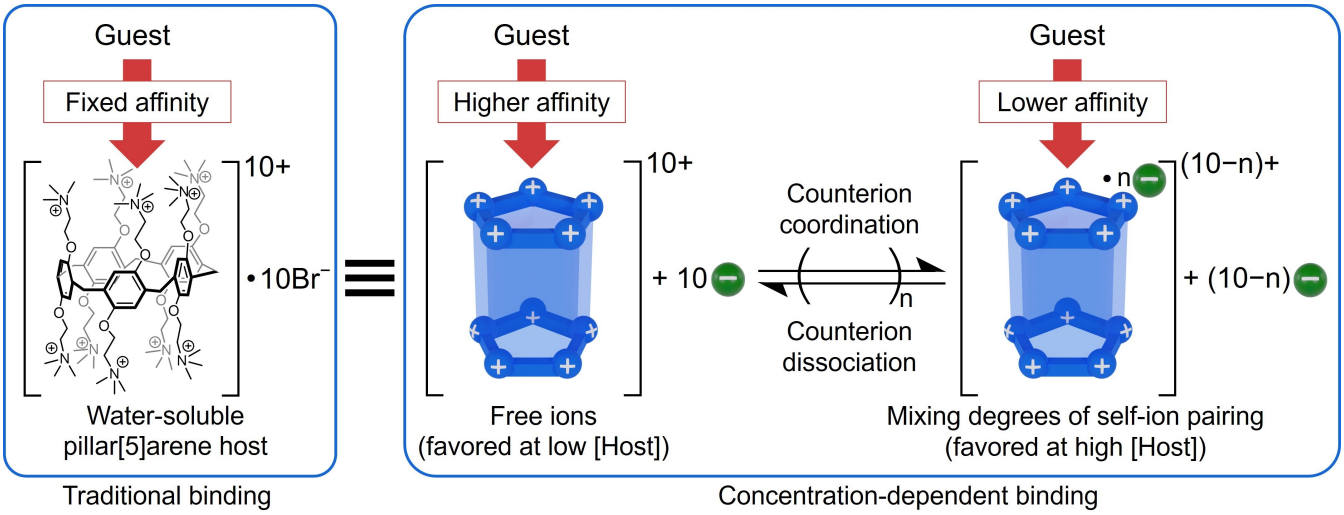

Scheme 1. Illustration depicting the initial hypothesis postulating the presence of different ionization states as a function of macrocycle concentration. This assumption proposes the existence of highly differentiated affinity levels for the formation of supramolecular complexes in those scenarios where electrostatic forces serve as the major driving force.

effective strategy to tune their solubility features.[60] Indeed, the introduction of charged moieties at the portals of these molecular receptors has proven to be a major advancement, enabling the use of these hosts in domains where their high aromaticity and low polarity would have otherwise posed a significant hurdle.[61] Hence, the selection of P5A appears to be an optimal choice for examining its ionization dynamics and affinity towards different guests over a broad range of concentrations in aqueous solution.

As aforementioned, one of the main challenges in using charged supramolecular receptors is the ubiquitous presence of their counterions, which not only alter the net charge of these hosts but also compete with the targeted guests for the complexation at the binding sites.[56,58,62–64] For this reason, as a preliminary step, it is necessary to determine the extent of the coordination of bromide ion to P5A within the concentration range under investigation. Only then can a rigorous analysis of the complexation capacity of this macrocycle be conducted. In this context, ion selective electrodes (ISE) offer an efficient means of determining these ionization states.[65] These electrodes selectively detect the activity of a given free ion, thereby allowing to quantify the extent of ion pairing in the equilibrium. In this way, it is possible to calculate the concentration of all these species involved and ultimately obtain the corresponding equilibrium constants and shed light on the molecular interactions at play.

Upon initial examination of the results produced by a bromide ion-selective electrode, it is apparent that the concentration of free $Br^-_{(aq)}$ across a wide range of concentrations of P5A is consistently lower than that expected for a strong electrolyte (Figure 1a). This difference becomes more pronounced as P5A concentration rises, providing evidence of a significant increase in self-ion pairing and consequently a higher rate of charge neutralization of the pillararene by its own counterion. The obtained results ultimately allow the calculation of the average number of counterions per pillararene molecule as a function of its concentration (Figure 1b). Herein, two distinct patterns are unveiled. On one hand, the number of counterions linked to the pillararene molecule remains roughly constant in the millimolar concentration range, with a value of five. This implies that five out of the ten coordination sites of the cationic pillararene are associated to a bromide ion, leading to a 50 % neutralization of the host's net charge. In simpler terms, the pillararene predominantly exists as $(P5ABr_5)^{5+}$. On the other hand, as the concentration decreases and shifts to the submillimolar regime, there is a dramatic decrease in the number of counterions associated to P5A. At this point, values as low as 0.26 are observed at 3.1×10^{-7} M, revealing that a mere 2.6 % of the coordination positions of the pillararene are occupied by bromide ions. This suggests that the charge of the pillararene remains largely unneutralized, mainly existing as $(P5A)^{10+}$. A comprehensive description of the data analysis for the estimation of these values can be found in Figure S1 and Scheme S1.

In order to provide additional support for the obtained results, lucigenin, a bromide-quenchable fluorescent probe commonly used to detect free halide ions, is employed (Figure S2). As detailed in Figure S3, a precise quantitative

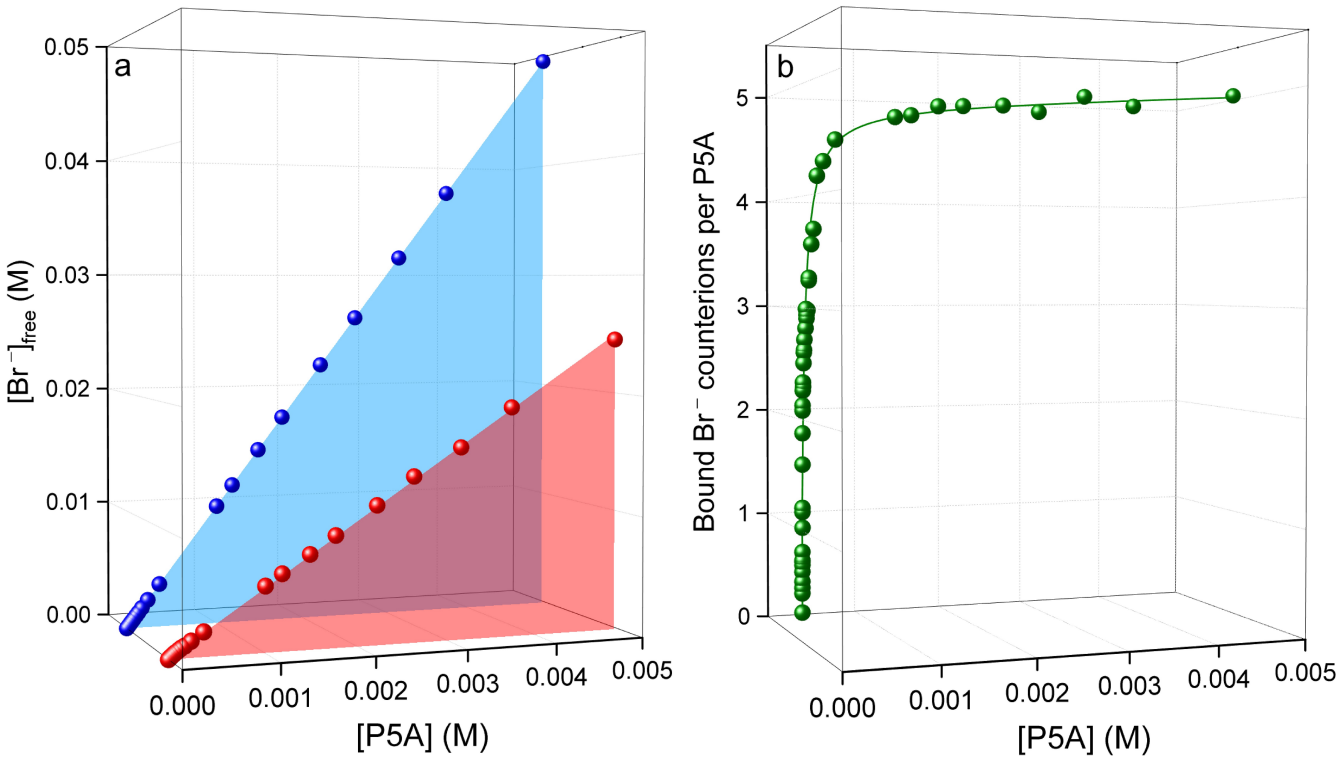

Figure 1. (a) Free bromide concentration in water as a function of P5A concentration (red) and expected trend in the absence of ion pairing (blue); and (b) average number of bound bromide counterions per pillararene molecule in water as a function of P5A concentration.

agreement is observed between the ratios of bound and free bromide ions determined using the fluorescence quenching methodology and those obtained through the utilization of an ion-selective electrode. This concordance confirms the reliability and accuracy of the results obtained using the latter. In this study, the ISE technique is predominantly employed due to its superior sensitivity compared to the fluorescence quenching method.

Keeping these results in mind, it becomes clear that P5A in solution is, in fact, a mixture of cationic macrocycles with varying fractions of neutralized charge. This array of receptors spans from the host with ten positive charges found in highly diluted samples, to its analog with five and even six bound bromides observed in more concentrated solutions. This is a matter of utmost importance, as it is logical to assume that upon formation of inclusion complexes with external anionic guests, $(P5A)^{10+}$ will give rise to stronger and more stable supramolecular assemblies than $(P5ABr_5)^{5+}$ and $(P5ABr_6)^{4+}$. At this stage, a model of complexation is proposed seeking to determine the equilibrium constants that govern the different ion-pairing processes occurring in the solution. This framework involves the sequential binding of six bromide ions to $(P5A)^{10+}$. In accordance with the results shown in Figure 1b, the extent of counterion coordination beyond 60 % is not considered. A schematic representation of the adopted complexation model together with the estimated equilibrium constants is depicted in Figure 2. A detailed account of the data analysis employed to determine these parameters is provided in the Supporting Information.

As shown in Figure 2, one can easily observe that reducing the net charge of the macrocycle triggers a substantial decline in the equilibrium constants, which exhibit a decrease of more than four orders of magnitude. Furthermore, upon determination of these constants, valuable insights can be gained into the abundance of each of these distinct supramolecular receptors as a function of the working concentrations. Figure 3 depicts the distribution of the different ionization states of these hosts in relation to P5A concentration. As can be observed, the pillararene exhibits highly variable charges depending on the dilution factor. At millimolar concentrations, the dominant form of the host is $(P5ABr_5)^{5+}$ which accounts for $\approx$80 % of the macrocycle. Although $(P5ABr_6)^{4+}$ shows an upward trend, it only makes a modest contribution in this range. As concentration decreases, a complex mixture of ionization states, including $(P5ABr_4)^{6+}$, $(P5ABr_3)^{7+}$, and $(P5ABr_2)^{8+}$, is found. Once in the submicromolar range, the prevailing form of the pillararene is $(P5A)^{10+}$ ($\approx$70 %), with a significant contribution from $(P5ABr)^{9+}$ ($\approx$30 %). In light of these trends, it becomes clear that the higher the dilution factor, the greater the charge of the species with the largest proportion.

This preliminary result is particularly interesting in terms of practical applications, as it is expected that electrostatic interactions will be the dominant driving force in the recognition of external anionic guests by these macrocycles. Moreover, the increasing ability of P5A to coordinate with its bromide counterions as its net charge increases further supports this notion, leading to infer that concentration, and by extension, the degree of ion pair formation, must be a critical parameter for the implementation of charged supramolecular receptors in aqueous media. In light of this, it is evident that the behavior of these macrocycles warrants careful consideration in the context of conducting complexation studies, as a variation in the concentration of the pillararene can induce a change in guest affinity.

At this point, the molecular recognition capabilities of this pillararene are explored. Given the polycationic nature of this receptor, p-toluenesulfonate (TS^-) is chosen as guest anion. Firstly, the complexation of P5A with TS^- is characterized through ^{1}H NMR titration experiments. With this aim, increasing concentrations of TS^- are added to a fixed concentration of P5A in order to analyze the change of the chemical shift of the signals corresponding to the anion. As depicted in Figure S4 and S5, a high-field shift of the TS^- methyl group signal is observed ($\Delta\delta = -3.32$ ppm). This is indicative of the formation of a P5A·TS^- complex where the aromatic ring is deeply embedded in the internal cavity of the pillararene. The stoichiometry of the resulting supramolecular assembly is verified by applying the mole-ratio method to the collected NMR datasets, unambiguously demonstrating the formation of a 1:1 host–guest complex (Figure S6 and S7). Electrospray ionization mass spectra offer additional validation of this binding mode, also delivering compelling evidence of the distinct electrostatic configurations that may be adopted by the macrocycle (Figure S8 and S9).

At this stage, the mechanism of formation of this supramolecular complex must be examined. For this purpose, a selective bromide ion electrode is employed, which allows us to draw conclusions about the nature of the process that takes place upon addition of the anionic guest. As shown in Figure 4a, the gradual incorporation of TS^- into the cavity of P5A induces the dissociation of the ion pairs established at the portals of the pillararene, resulting in the simultaneous release of one bromide ion upon incorporation of the tosylate ion into the cavity of the macrocycle. Similar conclusions can be drawn using lucigenin as a sensor of free bromide ions. As shown in Figure 4b, there is a decrease in the fluorescence intensity of this colorimetric probe in the presence of increasing concentrations of TS^- at a given concentration of P5A. This decline must be attributed to the release of bromide ions upon guest complexation and the subsequent interaction with lucigenin. This trend is equally observable in the presence of other inorganic anions (Figure S10 to S14), providing further evidence that guest recognition by P5A proceeds through an ion exchange process. In this context, the different extents to which this phenomenon occurs (Figure S15) underscore the significant influence of the nature of the ion on the wide array of behaviors that may be observed in these supramolecular systems and calls for a case-by-case analysis to fully understand the intricacies of these interactions.

Considering these results, the process of guest recognition by P5A must be understood as an exchange equilibrium in which the inclusion of the anionic guest involves the release of a counterion from the macrocycle and hence,

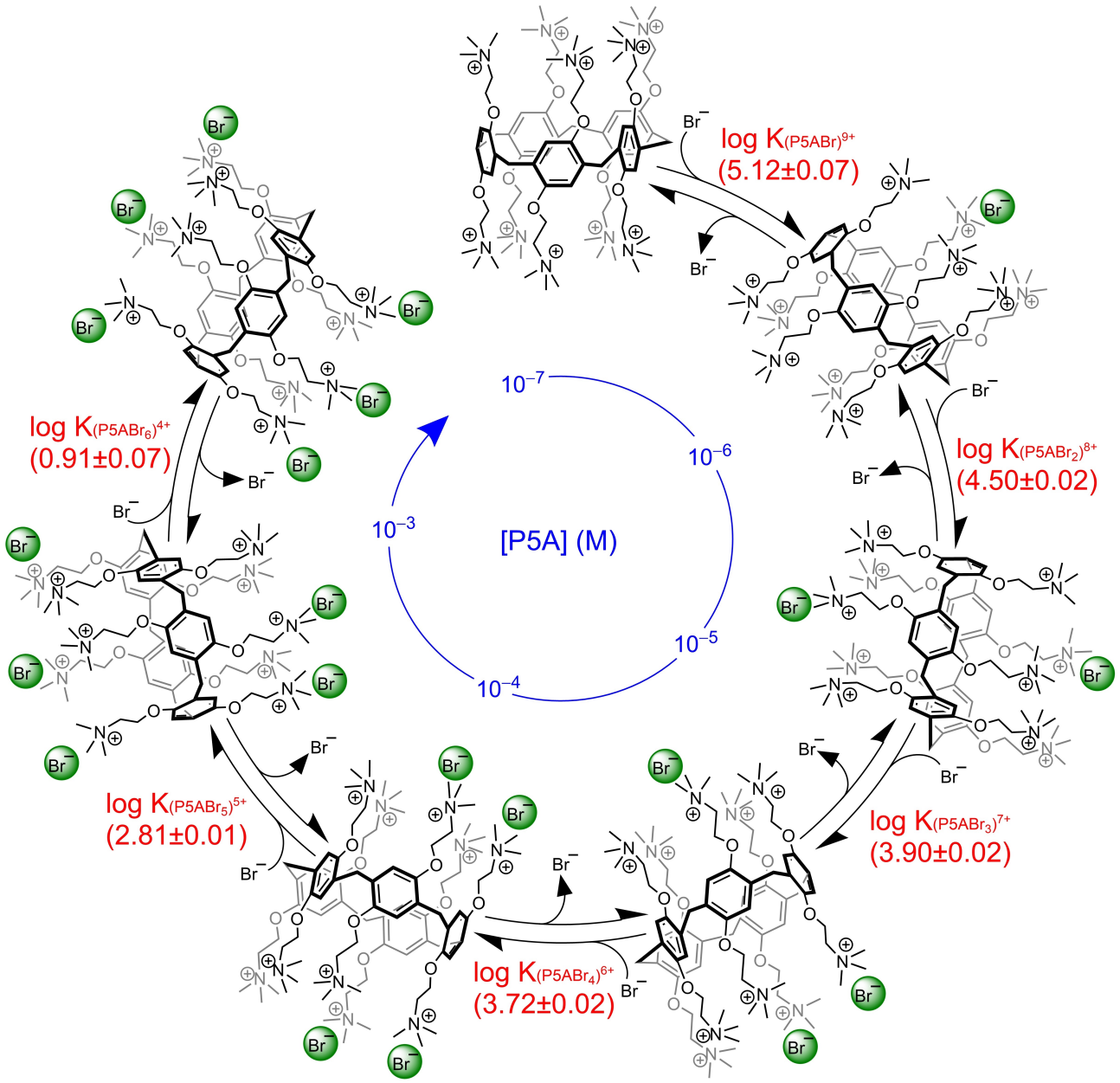

Figure 2. Mechanistic proposal representing the different degrees of ion pairing in water as a function of pillararene concentration. The equilibrium constants presented are determined by fitting the ISE data (Figure 1b) to the mass balance equations derived from this model (Equations [1] to [24] in the Supporting Information).

the preservation of the net charge of the pillararene (Scheme 2). In the same vein, the alterations detected in the ^{1}H NMR spectrum of the P5A·TS$^-$ complex in response to increasing concentrations of sodium bromide offer additional proof of this competitive phenomenon (Figure S16 and S17).

Having reached this point, it is necessary to quantify the extent to which this ion exchange process occurs depending on the charge adopted by the pillararene. To this end, isothermal titration calorimetry (ITC) experiments are performed over a concentration range of P5A spanning from 2.5×10^{-5} M to 4.5×10^{-3} M upon titration with TS$^-$ (Figure S18 to S23). It must be noted that these experiments are carried out by adding the guest to the sample cell containing the host to minimize potential changes in the concentration of P5A, which would result in a variation in the distribution of the different ionization states of the pillararene. In the defined interval, and as previously shown in Figure 3, P5A exists as a combination of $(P5ABr)^{9+}$, $(P5ABr_2)^{8+}$, $(P5ABr_3)^{7+}$, $(P5ABr_4)^{6+}$, and $(P5ABr_5)^{5+}$. Hence, to streamline the processing of the ITC data, a segmented analysis is conducted (Scheme S2). In the lower range of concentrations, P5A exhibits up to four different forms, namely $(P5ABr)^{9+}$, $(P5ABr_2)^{8+}$, $(P5ABr_3)^{7+}$, $(P5ABr_4)^{6+}$. Under this regime, ITC data are fitted to a mechanistic model in which the ion exchange only involves

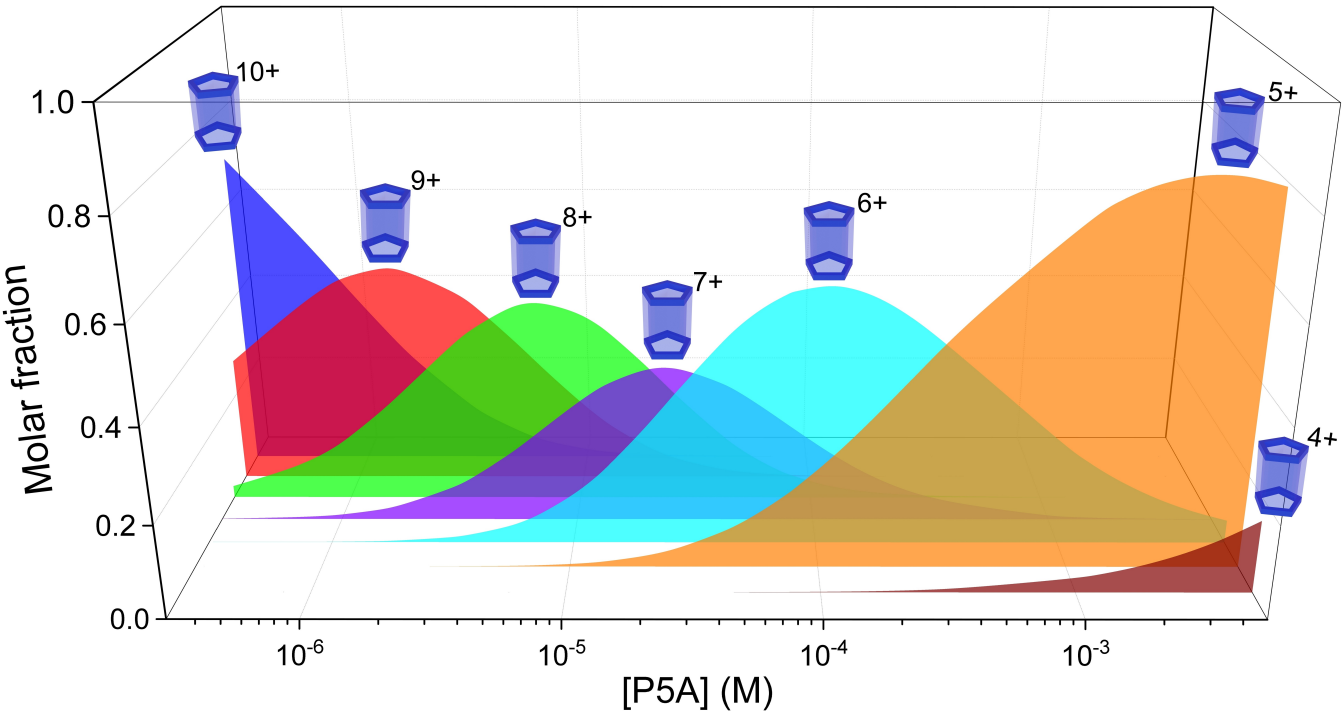

Figure 3. Distribution of the different ionization states of the pillararene in water as a function of P5A concentration. It can be observed that P5A transitions from a 10+ ionization state (absence of ion pairs) at submicromolar concentrations to a low-proportion 4+ ionization state (formation of six ion pairs) at millimolar concentrations. Throughout this range, several intermediate stages emerge where different forms coexist.

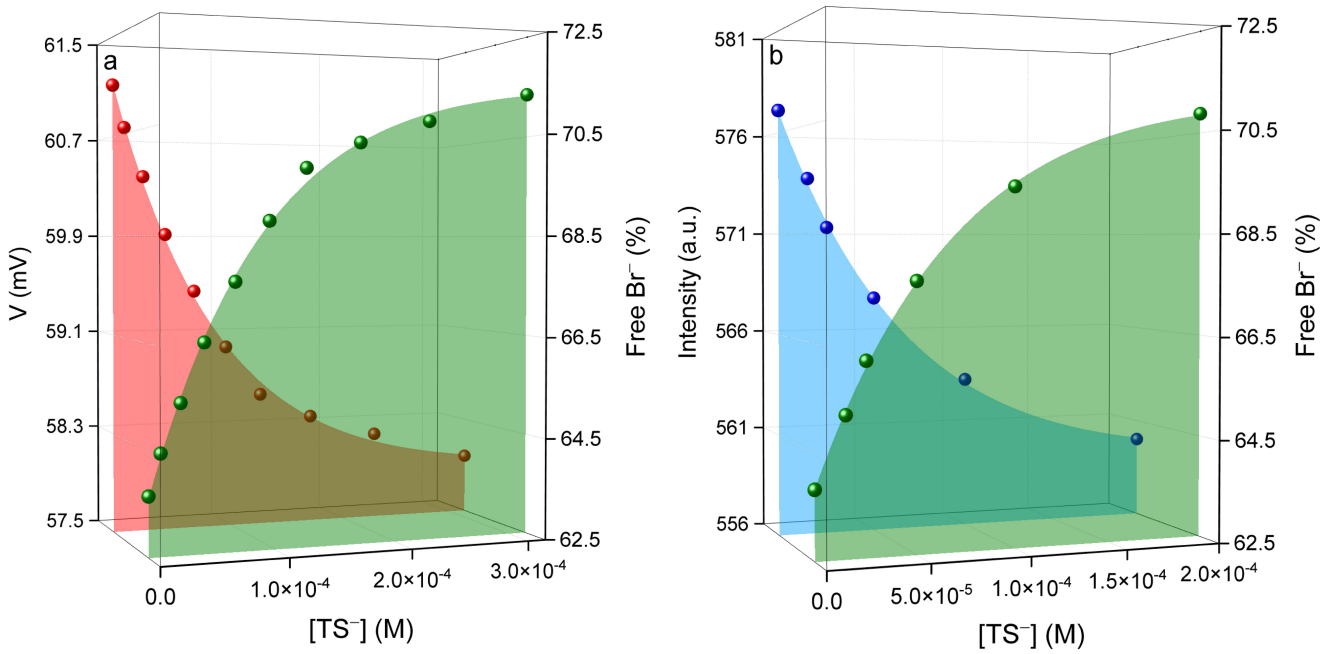

Figure 4. (a) Electrical potential of P5A (1.04×10^{-4} M) in water in the presence of increasing concentrations of sodium *p*-toluenesulfonate (red) and percentage of free bromide counterions as a function of TS^- concentration (green) derived from the curve of electrical potentials (Figure S1); and (b) fluorescence intensity of lucigenin (1×10^{-6} M) at 503 nm in water as a function of TS^- concentration in the presence of [P5A] = 1.04×10^{-4} M (blue) and resulting percentage of free bromide counterions as a function of TS^- concentration (green) obtained through the Stern–Volmer equation (Figure S2).

the participation of those macrocycles. In the higher range, the pillararene exists as a combination of $(P5ABr_2)^{8+}$, $(P5ABr_3)^{7+}$, $(P5ABr_4)^{6+}$, and $(P5ABr_5)^{5+}$. In this case, the model is refined to exclusively consider the contribution of

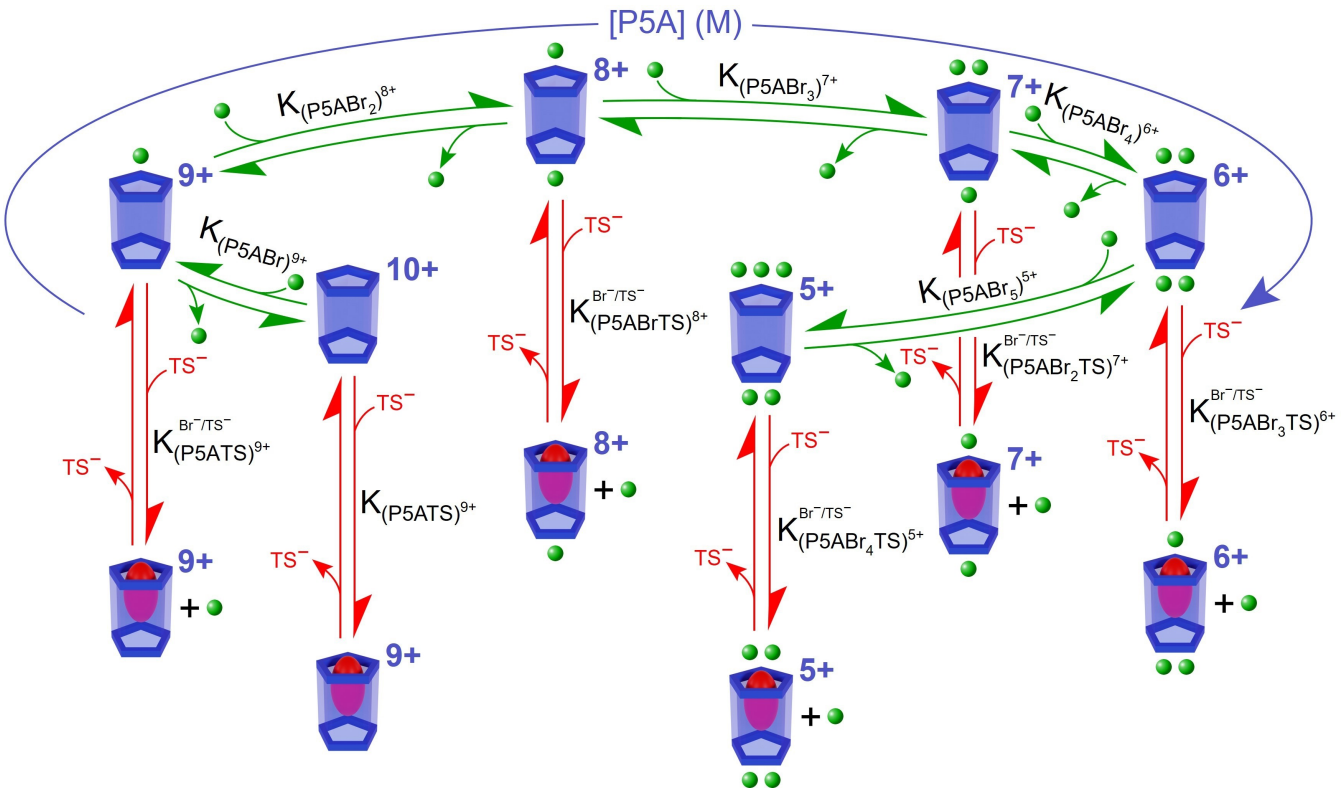

Scheme 2. Mechanism underlying the formation of the different supramolecular complexes between P5A and *p*-toluenesulfonate as a function of pillararene concentration. As illustrated, the inclusion of the guest molecule in the macrocycle arises from the interplay between the self-ion pairing of P5A and the ion-exchange process between the pillararene counterions and the guest.

those states in the ion exchange phenomenon, thereby neglecting the contribution of other forms. Through this sequential approach, a straightforward estimation of the ion exchange constants can be accomplished, as the outputs from the initial segment serve as inputs for the subsequent calculation. In this way, it is possible to determine the extent of Br^-/TS^- exchange at the portals of P5A as a function of its concentration. The resulting values for the ion exchange constants are presented in Table 1. As observed, in terms of magnitude the ion exchange constant remains relatively constant for the highly charged macrocycles, albeit with a slight decreasing trend. However, as the net charge of the pillararene decreases, a pronounced decline is observed. This decrease can be attributed to the diminished electrostatic attraction between the macrocycle and the anionic guest, primarily due to the formation of self-ion pairs at high concentrations of P5A.

To further validate the mechanism outlined in Scheme 2, attempts are made to fit these experimental data to a one-site binding model. A satisfactory fit to this framework would indicate that, regardless of the concentration, all the cavities of P5A have the same affinity for the guest they interact with and thus, TS^- should bind to the binding site of the pillararene with the same strength. As depicted in Figure S24 to S29, the ITC data clearly deviate from this behavior, providing compelling evidence for the concurrent presence of multiple binding sites in solution. This can be solely attributed to the existence of diverse ionization states in the macrocycle.

Table 1: (a) Equilibrium constants for the formation of P5A·Br^- self-ion pairs determined by fitting the ISE data to the mass balance equations (Equations [1] to [24] in the Supporting Information); (b) Equilibrium constants for the TS^-/Br^- ion exchange obtained through the ITC experiments performed upon titration of P5A with TS^- (Figure S18 to S23); (c) Binding constants for the formation of the supramolecular P5A·TS^- complexes calculated based on the aforementioned values (as explained in Scheme S3).

(a)	$K_{(P5ABr)^{9+}}$ (M^{-1})	$K_{(P5ABr_2)^{8+}}$ (M^{-1})	$K_{(P5ABr_3)^{7+}}$ (M^{-1})	$K_{(P5ABr_4)^{6+}}$ (M^{-1})	$K_{(P5ABr_5)^{5+}}$ (M^{-1})
	$(1.32\pm0.20)\times10^5$	$(3.16\pm0.18)\times10^4$	$(7.89\pm0.34)\times10^3$	$(5.25\pm0.21)\times10^3$	$(6.47\pm0.17)\times10^2$
(b)	$K^{Br^-/TS^-}_{(P5ATS)^{9+}}$	$K^{Br^-/TS^-}_{(P5ABrTS)^{8+}}$	$K^{Br^-/TS^-}_{(P5ABr_2TS)^{7+}}$	$K^{Br^-/TS^-}_{(P5ABr_3TS)^{6+}}$	$K^{Br^-/TS^-}_{(P5ABr_4TS)^{5+}}$
	$(2.90\pm0.06)\times10^6$	$(1.50\pm0.02)\times10^6$	$(1.30\pm0.01)\times10^6$	$(9.20\pm0.60)\times10^4$	$(5.60\pm0.40)\times10^2$
(c)	$K_{(P5ATS)^{9+}}$ (M^{-1})	$K_{(P5ABrTS)^{8+}}$ (M^{-1})	$K_{(P5ABr_2TS)^{7+}}$ (M^{-1})	$K_{(P5ABr_3TS)^{6+}}$ (M^{-1})	$K_{(P5ABr_4TS)^{5+}}$ (M^{-1})
	$(3.83\pm0.58)\times10^{11}$	$(4.74\pm0.28)\times10^{10}$	$(1.03\pm0.04)\times10^{10}$	$(4.83\pm0.37)\times10^8$	$(3.62\pm0.28)\times10^5$

At this stage, it is imperative to quantify the affinity of TS^- for P5A, considering that the pillararene may adopt different ionization states depending on its concentration, which logically must have a critical impact on the formation of supramolecular complexes where attractive interactions are the major driving force. A clear indication of the importance of the electrostatic charge in the formation of these host–guest complexes is found in Table 1, where a 10^4-fold decrease in the bromide ion association constant to P5A is shown when going from $(P5A)^{10+}$ to $(P5ABr_5)^{5+}$. By establishing a parallel with this behavior, it is expected that TS^- will exhibit greatly differentiated affinities depending on the charge of the host, or in other words, depending on the concentration of this molecular receptor. The binding constants of TS^- to the different configurations of P5A can be easily calculated through the product of the $P5A{\cdot}Br^-$ association constants and the Br^-/TS^- ion exchange constants (Scheme S3). The obtained $P5A{\cdot}TS^-$ complexation constants are shown in Table 1. As can be observed, the value corresponding to the formation of the $(P5ATS)^{9+}$ complex is over one million times higher than that obtained for the $(P5ABr_4TS)^{5+}$ complex. This finding confirms the hypothesis initially raised regarding the significant impact that the association of counterions has on the ability of P5A to encapsulate molecular guests. In this sense, as there is a shift from a millimolar to a micromolar concentration range, there is an increase in the net electrostatic charge of the macrocycle and hence, a great potentiation of its efficiency to accommodate anionic guests. Yet, it is essential to take into account that additional types of interactions may play a role in binding ions to the receptor's apolar cavity. In particular, tosylate ions are likely to benefit from aromatic and dispersion interplays, along with the hydrophobic effect, all of which can make substantial contributions to molecular recognition. Still, these interactions remain consistent across all the different electrostatic configurations of P5A.

The significant variability in the formation constants of $P5A{\cdot}TS^-$ depending on P5A concentration and thus, the ionization state of this macrocycle, opens interesting scenarios in terms of applications. Notably, the dilution of these supramolecular receptors may even enhance their hosting capacity, leading to a counterintuitive observation where a three-order-of-magnitude decrease in the host concentration can lead to a slight increase in the amount of the guest accommodated within the pillararene cavity (Scheme S4). This would suggest that, in practical contexts, the required operational concentrations of polyionic hosts have often been overestimated. Consequently, by maximizing the complexation capabilities of P5A at concentration ranges that do not favor ion pair formation, the impact of high dilution can be offset, resulting in highly efficient supramolecular systems in aqueous solution. Along these lines, it should be noted that to the best of our knowledge, the binding constant obtained for $(P5A)^{10+}$ ($3.83\times10^{11}\ M^{-1}$) is one of the largest values ever reported for a pillararene or its derivatives in aqueous solution.[66]

The fact that the concentration of the host plays such a crucial role in this context reveals the deterministic nature of estimating binding constants in host–guest chemistry. It is important to note that, in order to evaluate the binding strength in supramolecular systems, a multitude of experimental techniques have traditionally been employed, including isothermal titration calorimetry, nuclear magnetic resonance, fluorescence, and UV/Visible spectroscopy.[67] Nevertheless, the sensitivity of these techniques differs significantly, resulting in substantial variations in the amount of analyte required for each method. In the case of multicharged hosts, this may lead to the determination of the same binding constant under different concentration regimes depending on the specific technique employed. An illustrative example highlighting the deterministic problem at hand can be provided by examining the inherent limitations of NMR spectroscopy. As known, this technique typically requires the use of a few milligrams for small molecules (<1000 g/mol), thereby implying that data acquisition generally occurs within the millimolar concentration range. In the present case, this requirement would pose a significant challenge since it would limit the analysis to $(P5ABr_5)^{5+}$, disregarding the various ionization states that may arise when working with P5A under alternative operational conditions. UV/Visible spectroscopy may afford higher sensitivities than those provided by NMR. Yet, absorption bands may saturate at relatively high concentrations, limiting the study to the ionization states within the narrow range of concentrations of this technique. Along these lines, the wide sensitivity range of ITC (from nanomolar to micromolar) renders this technique ideal to address the dynamic nature of these systems, enabling a more comprehensive understanding of perfunctionalized macrocycles.

The deterministic nature of the measurements of the affinity constant is not only limited to the instrumental techniques employed, but also to the experimental design itself. Typically, the most common approach to determine the binding affinity of a guest for a host involves varying the concentration of one component while keeping constant the concentration of the other binding partner. In the case of multicharged receptors, this experimental design may result in alterations in the electrostatic charge of the host as the measurement progresses. This would render it unfeasible to provide a value for the affinity constant as the host would exhibit a changing nature throughout the experiment. The issue of the variability of the electrostatic configuration of the host is further compounded by the possible coexistence of different ionization states, particularly in intermediate concentration regimes, which greatly hampers the calculation of binding constants, as it becomes necessary to discriminate between the different forms of the host that are simultaneously present in solution.

Conclusion

The present study unveils the significant variability in supramolecular binding constants when employing multicharged receptors. These notable alterations in the affinity values are driven by the formation of self-ion pairs depending on the host concentration, leading to a change in the net charge of the host, which in turn exerts a profound impact

on the formation of those host–guest complexes where electrostatic interactions serve as the major driving force. The results obtained in this study shed light on the deterministic nature underlying the estimation of association constants, heavily influenced by the sensitivity of the instrumental technique employed. Furthermore, based on the achieved results, it is evident that the design of experiments aimed at determining supramolecular binding constants must be carefully formulated to avoid variations in the concentration of these polyionic hosts. Failure to do so could lead to misleading conclusions due to the dynamic nature of these species. The findings derived from this investigation call for a critical reassessment of the existing data pertaining to multicharged hosts, emphasizing the need to explicitly specify concentration as a key element when reporting the complexation ability of these supramolecular receptors. Also, considering the significant potential of polyionic hosts for practical applications, it becomes clear that conducting a comparative evaluation of different synthetic receptors in buffered solutions with a high concentration of competing ions is essential. Consequently, those receptors displaying a strong affinity for the target guest molecules under these challenging conditions should be identified as the most promising candidates for their intended use.

Acknowledgements

This work was funded by Ministerio de Ciencia e Innovación (PID2020-113704RB-I00), and Xunta de Galicia (Centro Singular de Investigación de Galicia-Accreditation 2019-2022 ED431G 2019/06, ED431C 2022/24, and ED431C 2021/45).

Conflict of Interest

The authors declare no conflict of interest.

Data Availability Statement

The data that support the findings of this study are available in the supplementary material of this article.

Keywords: Host-Guest · Ion-Pairing · Macrocycle · Pillararene · Supramolecular Affinity

[1] J. F. Woods, L. Gallego, P. Pfister, M. Maaloum, A. Vargas Jentzsch, M. Rickhaus, *Nat. Commun.* **2022**, *13*, 3681.
[2] J. M. Cameron, G. Guillemot, T. Galambos, S. S. Amin, E. Hampson, K. Mall Haidaraly, G. N. Newton, G. Izzet, *Chem. Soc. Rev.* **2022**, *51*, 293–328.
[3] Y. Yao, Q. Ou, K. Wang, H. Peng, F. Fang, Y. Shi, Y. Wang, D. I. Asperilla, Z. Shuai, P. Samorì, *Nat. Commun.* **2021**, *12*, 3667.
[4] Y. Wang, X. Huang, X. Zhang, *Nat. Commun.* **2021**, *12*, 1291.
[5] G. Fang, X. Yang, S. Chen, Q. Wang, A. Zhang, B. Tang, *Coord. Chem. Rev.* **2022**, *454*, 214352.
[6] S. Bernhard, M. W. Tibbitt, *Adv. Drug Delivery Rev.* **2021**, *171*, 240–256.
[7] C. Xu, B. Yu, Y. Qi, N. Zhao, F.-J. Xu, *Adv. Healthcare Mater.* **2021**, *10*, 2001183.
[8] W.-C. Geng, J. L. Sessler, D.-S. Guo, *Chem. Soc. Rev.* **2020**, *49*, 2303–2315.
[9] Y. Sasaki, X. Lyu, W. Tang, H. Wu, T. Minami, *J. Photochem. Photobiol. C* **2022**, *51*, 100475.
[10] C. Guo, A. C. Sedgwick, T. Hirao, J. L. Sessler, *Coord. Chem. Rev.* **2021**, *427*, 213560.
[11] G. Fukuhara, *J. Photochem. Photobiol. C* **2020**, *42*, 100340.
[12] R. Hein, P. D. Beer, J. J. Davis, *Chem. Rev.* **2020**, *120*, 1888–1935.
[13] B. Xie, Y.-F. Ding, M. Shui, L. Yue, C. Gao, I. W. Wyman, R. Wang, *Eur. J. Nucl. Med. Mol. Imaging* **2022**, *49*, 1200–1210.
[14] Y. Deng, W. Zhan, G. Liang, *Adv. Healthcare Mater.* **2021**, *10*, 2001211.
[15] W.-L. Zhou, Y. Chen, Q. Yu, H. Zhang, Z.-X. Liu, X.-Y. Dai, J.-J. Li, Y. Liu, *Nat. Commun.* **2020**, *11*, 4655.
[16] X. Mu, Y. Lu, F. Wu, Y. Wei, H. Ma, Y. Zhao, J. Sun, S. Liu, X. Zhou, Z. Li, *Adv. Mater.* **2020**, *32*, 1906711.
[17] R. Saha, B. Mondal, P. S. Mukherjee, *Chem. Rev.* **2022**, *122*, 12244–12307.
[18] P. M. Stanley, J. Haimerl, C. Thomas, A. Urstoeger, M. Schuster, N. B. Shustova, A. Casini, B. Rieger, J. Warnan, R. A. Fischer, *Angew. Chem. Int. Ed.* **2021**, *60*, 17854–17860.
[19] T. Keijer, T. Bouwens, J. Hessels, J. N. H. Reek, *Chem. Sci.* **2021**, *12*, 50–70.
[20] M. Morimoto, S. M. Bierschenk, K. T. Xia, R. G. Bergman, K. N. Raymond, F. D. Toste, *Nat. Catal.* **2020**, *3*, 969–984.
[21] H.-B. Cheng, H. Dai, X. Tan, H. Li, H. Liang, C. Hu, M. Huang, J. Y. Lee, J. Zhao, L. Zhou, Y. Wang, L. Zhang, J. Yoon, *Adv. Mater.* **2022**, *34*, 2109111.
[22] J. Zhou, L. Rao, G. Yu, T. R. Cook, X. Chen, F. Huang, *Chem. Soc. Rev.* **2021**, *50*, 2839–2891.
[23] K. Wang, K. Velmurugan, B. Li, X.-Y. Hu, *Chem. Commun.* **2021**, *57*, 13641–13654.
[24] M. R. Wasielewski, M. D. E. Forbes, N. L. Frank, K. Kowalski, G. D. Scholes, J. Yuen-Zhou, M. A. Baldo, D. E. Freedman, R. H. Goldsmith, T. Goodson, M. L. Kirk, J. K. McCusker, J. P. Ogilvie, D. A. Shultz, S. Stoll, K. B. Whaley, *Nat. Chem. Rev.* **2020**, *4*, 490–504.
[25] S. Sarkar, P. Ballester, M. Spektor, E. A. Kataev, *Angew. Chem. Int. Ed.* **2023**, *62*, e202214705.
[26] Q. Shi, X. Wang, B. Liu, P. Qiao, J. Li, L. Wang, *Chem. Commun.* **2021**, *57*, 12379–12405.
[27] W. Liu, J. F. Stoddart, *Chem* **2021**, *7*, 919–947.
[28] Y.-M. Zhang, Y.-H. Liu, Y. Liu, *Adv. Mater.* **2020**, *32*, 1806158.
[29] J. Wankar, N. G. Kotla, S. Gera, S. Rasala, A. Pandit, Y. A. Rochev, *Adv. Funct. Mater.* **2020**, *30*, 1909049.
[30] Z. Wang, C. Sun, K. Yang, X. Chen, R. Wang, *Angew. Chem. Int. Ed.* **2022**, *61*, e202206763.
[31] Y.-H. Liu, Y.-M. Zhang, H.-J. Yu, Y. Liu, *Angew. Chem. Int. Ed.* **2021**, *60*, 3870–3880.
[32] E. Masson, X. Ling, R. Joseph, L. Kyeremeh-Mensah, X. Lu, *RSC Adv.* **2012**, *2*, 1213–1247.
[33] Y.-C. Pan, X.-Y. Hu, D.-S. Guo, *Angew. Chem. Int. Ed.* **2021**, *60*, 2768–2794.
[34] X. Fan, X. Guo, *J. Mol. Liq.* **2021**, *325*, 115246.
[35] T.-H. Shi, S. Ohtani, K. Kato, S. Fa, T. Ogoshi, *Trends Chem.* **2023**, https://doi.org/10.1016/j.trechm.2023.04.004.
[36] X. Xu, V. V. Jerca, R. Hoogenboom, *Angew. Chem. Int. Ed.* **2020**, *59*, 6314–6316.
[37] Y. Fang, Y. Deng, W. Dehaen, *Coord. Chem. Rev.* **2020**, *415*, 213313.

[38] L. Escobar, P. Ballester, *Chem. Rev.* **2021**, *121*, 2445–2514.
[39] L. Yue, K. Yang, X.-Y. Lou, Y.-W. Yang, R. Wang, *Matter* **2020**, *3*, 1557–1588.
[40] C.-L. Deng, S. L. Murkli, L. D. Isaacs, *Chem. Soc. Rev.* **2020**, *49*, 7516–7532.
[41] M. A. Beatty, F. Hof, *Chem. Soc. Rev.* **2021**, *50*, 4812–4832.
[42] Z. Liu, Y. Liu, *Chem. Soc. Rev.* **2022**, *51*, 4786–4827.
[43] J. Murray, K. Kim, T. Ogoshi, W. Yao, B. C. Gibb, *Chem. Soc. Rev.* **2017**, *46*, 2479–2496.
[44] Y. Liu, F. Zhou, F. Yang, D. Ma, *Org. Biomol. Chem.* **2019**, *17*, 5106–5111.
[45] G. Szalóki, V. Croué, V. Carré, F. Aubriet, O. Alévêque, E. Levillain, M. Allain, J. Aragó, E. Ortí, S. Goeb, M. Sallé, *Angew. Chem. Int. Ed.* **2017**, *56*, 16272–16276.
[46] G. Szalóki, V. Croué, M. Allain, S. Goeb, M. Sallé, *Chem. Commun.* **2016**, *52*, 10012–10015.
[47] D. P. August, G. S. Nichol, P. J. Lusby, *Angew. Chem. Int. Ed.* **2016**, *55*, 15022–15026.
[48] S. Kubik, *ChemistryOpen* **2022**, *11*, e202200028.
[49] N. F. A. van der Vegt, K. Haldrup, S. Roke, J. Zheng, M. Lund, H. J. Bakker, *Chem. Rev.* **2016**, *116*, 7626–7641.
[50] Y. Marcus, G. Hefter, *Chem. Rev.* **2006**, *106*, 4585–4621.
[51] S. Yadav, A. Chandra, *J. Chem. Phys.* **2017**, *147*, 244503.
[52] E. H. Wanderlind, D. G. Liz, A. P. Gerola, R. F. Affeldt, V. Nascimento, L. C. Bretanha, R. Montecinos, L. Garcia-Rio, H. D. Fiedler, F. Nome, *ACS Catal.* **2018**, *8*, 3343–3347.
[53] X. Sun, B. Li, D. Wan, N. Wang, *J. Environ. Sci.* **2016**, *50*, 3–12.
[54] S. He, B. Huang, B. Xiao, S. Chang, M. Podalko, W. M. Nau, *Angew. Chem. Int. Ed.* **2023**, *62*, e202313864.
[55] C. Hu, T. Jochmann, P. Chakraborty, M. Neumaier, P. A. Levkin, M. M. Kappes, F. Biedermann, *J. Am. Chem. Soc.* **2022**, *144*, 13084–13095.
[56] J. H. Jordan, H. S. Ashbaugh, J. T. Mague, B. C. Gibb, *J. Am. Chem. Soc.* **2021**, *143*, 18605–18616.
[57] S. Zhang, L. Grimm, Z. Miskolczy, L. Biczók, F. Biedermann, W. M. Nau, *Chem. Commun.* **2019**, *55*, 14131–14134.
[58] V. Francisco, A. Piñeiro, W. M. Nau, L. García-Río, *Chem. Eur. J.* **2013**, *19*, 17809–17820.
[59] Y. Ma, X. Ji, F. Xiang, X. Chi, C. Han, J. He, Z. Abliz, W. Chen, F. Huang, *Chem. Commun.* **2011**, *47*, 12340–12342.
[60] N. L. Strutt, H. Zhang, S. T. Schneebeli, J. F. Stoddart, *Acc. Chem. Res.* **2014**, *47*, 2631–2642.
[61] H. Zhu, Q. Li, L. E. Khalil-Cruz, N. M. Khashab, G. Yu, F. Huang, *Sci. China Chem.* **2021**, *64*, 688–700.
[62] S. Fernández-Abad, M. Pessêgo, N. Basílio, L. García-Río, *Chem. Eur. J.* **2016**, *22*, 6466–6470.
[63] V. Francisco, N. Basílio, L. García-Río, *J. Phys. Chem. B* **2014**, *118*, 4710–4716.
[64] V. Francisco, N. Basilio, L. García-Río, *J. Phys. Chem. B* **2012**, *116*, 5308–5315.
[65] S. Suman, R. Singh, *Microchem. J.* **2019**, *149*, 104045.
[66] W. Xue, P. Y. Zavalij, L. Isaacs, *Angew. Chem. Int. Ed.* **2020**, *59*, 13313–13319.
[67] P. Thordarson, *Chem. Soc. Rev.* **2011**, *40*, 1305–1323.

Manuscript received: November 17, 2023
Accepted manuscript online: December 15, 2023
Version of record online: January 10, 2024